Size Anisotropy Inhomogeneity Effects in State-of-the-Art Quantum Dot Lasers

I.M.E. Butler[a)]
School of Engineering, University of Glasgow, Glasgow, G12 8LT, UK and
School of Mathematics and Physics, Queens University Belfast, Belfast, BT7 1NN, UK
Wei Li
Department of Electronic & Electrical Engineering, University of Sheffield, Sheffield, S1 4DE, UK
S.A. Sobhani and N. Babazadeh
School of Engineering, University of Glasgow, Glasgow, G12 8LT, UK
I.M. Ross
Department of Electronic & Electrical Engineering, University of Sheffield, Sheffield, S1 4DE, UK
K. Nishi, K. Takemasa, and M. Sugawara
QD Laser Inc, Keihin Bldg. 1F, 1-1 Minamiwataridacho, Kawasaki-ku, Kawasaki, Kanagawa 210-0855, JAPAN
D.T.D. Childs and R.A. Hogg
School of Engineering, University of Glasgow, Glasgow, G12 8LT, UK

(Dated: January 2018; Revised May 2018)

We describe a high angle annular dark field scanning transmission electron microscopy (HAADF STEM) study of self-assembled InAs-GaAs quantum dot (QD) laser sample, providing insight into the micro-structure of the QD ensemble. A size distribution anisotropy of the QDs is observed in the two orthogonal (110) planes, this structural information is used to develop a density of states model for the QD ensemble which is shown to be in strong agreement with a range of optical spectroscopic measurements. This link between micro-structure and optical properties allow routes to QD device simulation. We go on to discuss how changes to the micro-structure would affect the density of states and hence laser performance.

Stranski-Krastanov (S-K) quantum dot (QD) lasers[1] have been an active research area for more than 30 years due to the prediction[2] and realisation[3,4] of temperature insensitive operation due to their delta-like density of states. The development of epitaxial processes has allowed GaAs based QDs to cover the ≈1.2[5] to 1.55μm range[6,7], that is not easily accessible by typical quantum well structures. In addition to achieving long wavelength emission, the control of inhomogeneous broadening of the QD ensemble is critical for high efficiencies[8] and high speed modulation[9]. Additionally, QDs been shown to reduce defects in the growth of GaAs based materials on silicon[10], paving the way to silicon photonics applications[11].

A reduction in the inhomogeneous linewidth can be monitored via spectroscopic methods such as photoluminescence (PL), photocurrent (PC) and photoluminescence excitation (PLE)[12–14]. A higher uniformity of dots results in lower inhomogeneous broadening resulting in smaller QD ensemble linewidths (<20meV)[15]. The micro-structure of QDs have been investigated through different microscopy techniques. While scanning tunnelling and atomic force microscopy is an easy method to see the microscopic structure of uncapped QDs, there is a clear issue in micro-structural knowledge of the capped QDs. Transmission electron microscopy (TEM) has been shown to provide vital information about QD shape and compositional uniformity[5].

Rigorous methods of QD simulation have been developed and discussed[16,17] and advanced TEM imaging of individual QDs has been made[18–20], but a link between the micro-structural characteristics of the QD ensemble, its opto-electronic characteristics, and hence device performance is timely. In particular, this would enable the simulation of gain spectra for the QD ensemble through Monte-carlo methods[21,22] In this letter we report a TEM study of self-assembled QDs embedded within the epitaxial structure which shows a QD size anisotropy along the two orthogonal [110] directions. A density of states (DoS) model for the ensemble is developed using structural information from TEM images. The results are found to be in agreement with low temperature electroluminescence (EL) and room temperature PC spectroscopy. Furthermore the effects of removing the identified inhomogeneity on the opto-electronic properties of QDs are discussed. This highlights a possible unmet challenge in QD epitaxy that if solved may results in future generations of QD based devices.

The QD sample was grown utilising standard processes using a solid-source molecular beam epitaxy (MBE) growth reactor, using a GaAs substrate, grown on the (100) plane. Each QD layer was created by the

[a)]Electronic mail: Iain.Butler@glasgow.ac.uk

deposition of InAs to form S-K InAs islands, which were encapsulated using an InGaAs strain reducing layer[13,23] and GaAs barriers which have a total combined thickness of ≈40nm. The active region is sandwiched between n- and p-doped AlGaAs cladding layers, to provide optical confinement and electrical injection. Full details of the growth process are described elsewhere[5,11,13]. These such structures find application in cooler-free tele- and data-communications Fabry-Pérot lasers upto 2.5Gbps.

Figure 1 (a) and (b) shows the high angle annular dark field scanning transmission electron microscopy (HAADF STEM) images of the minor flat (a) and the major flat (b), showing 6 layers (out of 10 layers) of the QD active region layers. Cross-sectional STEM samples were prepared along the two orthogonal (110) planes in-correlation with the conventional grinding and mechanical polishing methods for creating minor $(0\bar{1}1)$ and major flats $(01\bar{1})$. This was achieved by argon ion milling at an acceleration voltage of 3kV and incident angle between 6°and 12°until hole perforation was achieved. In this work, the specimen thickness at the region of interest was estimated from analysis of the local zero energy-loss spectrum to ensure regions of similar thickness were selected for measurement. HAADF STEM z-contrast images were acquired with a JEOL R005 aberration corrected TEM/STEM operating at 300kV with a convergence semi-angle of 21mrads and a STEM inner annular collection angle of 62mrads.

Using HAADF STEM, intensity profiles provide information about the distribution of indium within the sample. HAADF intensity is approximately proportional to the square of Z, leading to changes in contrast where the electron beam has been deflected due to the changes in composition. InAs and GaAs have a clear contrast difference due to the differences between their atomic numbers (indium =49, gallium =31), with indium appearing brighter compared to gallium[18]. The labels added to Fig. 1 (a) indicate the regions of the sample; the GaAs buffer layer, the QD and the wetting layer/strain reducing layer (WL/SRL).

Figure 1 (c) shows the QD width distribution measured in the two orthogonal (110) planes. QD widths were measured using the full width half maximum (FWHM) of the integrated intensity profile. Each QD was measured individually, with an example shown in the inset for two neighbouring QDs in the minor flat plane, with both example QDs showing a FWHM of approximately 20nm. The width distribution was measured over a total of 150 QDs. The results for the two orthogonal (110) planes are shown with bin sizes of 2nm. The standard deviation is 2nm (6nm), with a mean value of 21.4nm (20.2nm) for the major (minor) flat respectively. This shows that there is a size distribution anisotropy in the two orthogonal [110] directions. The cause of this anisotropy is not yet understood, but may result from the non-equivalence of the [110] directions during epitaxy[24], and/or an anisotropic diffusion of indium during capping[25].

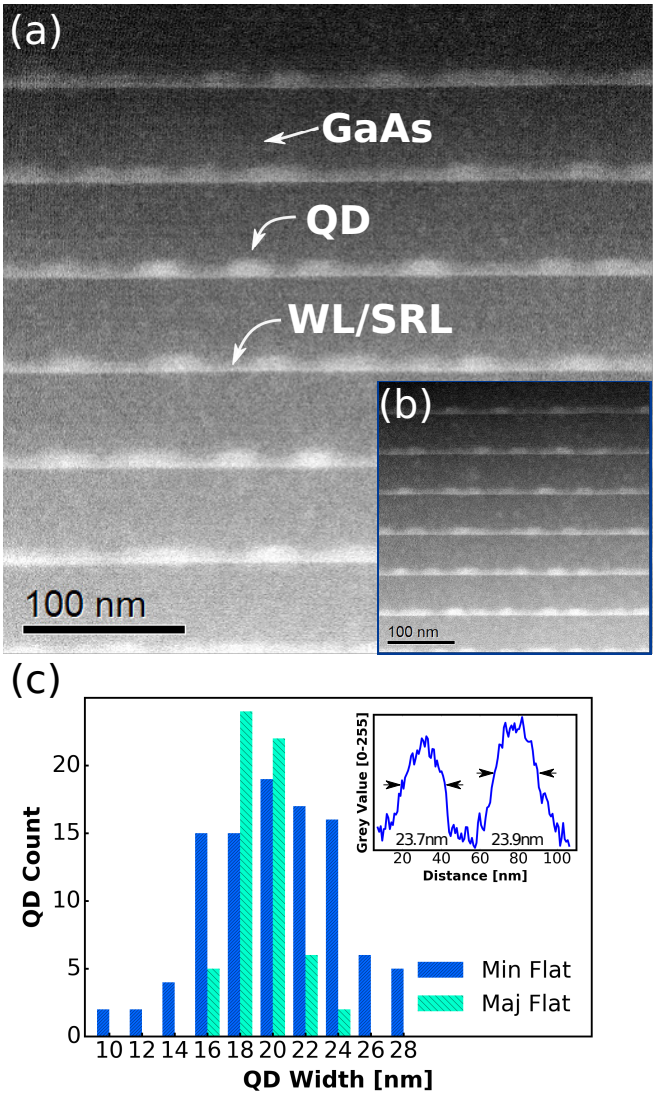

FIG. 1: (a) HAADF STEM image of the minor flat QD laser sample active region. The substrate (GaAs), the QD and the wetting layer/strain reducing layer (WL/SRL) is labelled. Vertical direction is growth direction and lateral is parallel to the sample surface (100). (b) HAADF STEM image of the major flat. (c) Quantum dot width distributions in (110) orthogonal planes. Inset shows an averaged pixel profile plot over 2 quantum dots.

In order to model the shape of the DoS of the QD ensemble, we consider the QDs electronic states to be described by using the particle in a box model (a solution to Schrödingers time-independent equation assuming infinite potential barriers). Infinite potentials is used for simplicity. Each QD is assumed to be made up of a uniform InGaAs alloy, as pure InAs QD are not realised practically[18]. The effective mass is a linear interpolation of the values for the binary alloys, selected and adjusted using the indium concentration. In simulating the ensemble we build up a probability matrix

matching the QD size distributions shown in figure 1, assuming no correlation between QD widths in the two orthogonal dimensions. That is to say for a given width in one plane, the width in the orthogonal dimension will have a width probability equal to the distribution in Fig. 1. The form of the ensemble DoS is then deduced by calculating the solution to Schrödingers equation in 3D using these QD dimensions. The QD height is assumed to be unchanged at 7nm[5]. The shape of the DoS is visualised by summing the confinement energies due to electrons and holes.

A good fit to spectroscopic data for these QDs was obtained using an indium concentration of 80%. An indium composition of 80% yielded transition energies for both the ground state (GS) and first excited state (ES) energies in good agreement with spectroscopic data[26], and is in-line with previous TEM studies[18,27]. The shape of the DoS of the first allowed (parity conserving) transition between the electron n_x=1 n_y=1 n_z=1 state and the hole n_x=1 n_y=1 n_z=1 state (where n= quantum number), corresponding to the QD GS is visualised by summing the calculated energies into equal energy bins and is shown in figure 2. In the following, transition n_x n_y n_z refers to the allowed (parity conserving) transitions between electron n_x n_y n_z and hole n_x n_y n_z states. The GS is therefore defined as 111.

EL measurements were conducted on a commercially available packaged QD laser structure consisting of 8 QD layers. The laser ridge has a width of 2μm and length 375μm. In order to investigate the form of the GS DoS, the laser is electrically driven using a current of 50 μA, providing an estimated average of 0.01 electron-hole pairs per QD. The environmental temperature is controlled using a cryogenic system. A standard dispersion monochromator with spectral resolution of 1nm was used.

Also plotted in Fig. 2 is the low QD occupancy EL from laser structures obtained at 15K, and has a linewidth of 45meV and peak emission energy of 1.04eV. Under these, low temperature (random population) and low current (excited states unlikely), conditions the measured spectrum can be considered to be a close approximation of the density of states for the ground-state transition as QD occupancy should be random, and the chance of multi-e-h pair occupancy is very low. A very good agreement between simulation and the experimental results is found in terms of the shape of the asymmetry of the QD GS DoS. Whilst we have a comparatively large number of measurements of the QD dimensions, the resultant granularity of the energy bins could be improved with further TEM analysis.

Figure 2 also shows the low QD occupancy EL at a temperature of 300K. The spectrum has a linewidth of 39meV and peak emission energy of 0.96eV. At higher temperatures the determination of QD carrier statistics is non-trivial[28], and this critical detail will modify the form of the EL spectrum. This uncertainty notwithstanding, we note that the EL spectrum shows an asymmetry, with a tail to higher energies. When a bimodal QD size distribution is present, two Gaussian functions should fit the spectra[29]. However we find that the EL spectra over a range of temperatures are not well fitted using two Gaussian functions.

Figure 3 shows room temperature (≈300K) PC responsivity for similar samples to the laser diodes described previously. PC is used as it provides a spectrum that approximates the absorption spectrum of the QDs. Whilst from different growth runs, the material had identical structure (8 QD layers), and was deposited using the same epitaxial process. This material was fabricated into optical access mesa diodes. The PC spectra were taken using spectrally filtered white light (resolution of 2nm) incident normal to the wafer surface. The light was chopped, and PC signal obtained using standard lock-in techniques. The responsivity was corrected for variations in incident optical power as a function of wavelength. A source-measurement unit was used to apply a 0V DC voltage across the device, in the growth direction. RT PC is a measure of the shape of the absorption spectrum and hence DoS if the escape of photo-created carriers is not a function of the excitation energy.

PC responsivity shows 2 peaks with a distinct non-zero valley. The first peak is found at 0.98eV and the second at 1.06eV, with a respective width of 24meV and 48meV are found using the FWHM of Gaussian fits. The responsivity is greater in the first compared to the second peak. The peak at 0.98eV is attributed to the GS and the peak at 1.06eV is attributed to the first ES.

It is expected that in a QD sample with in-plane symmetry, the first ES transition would exhibit double the degeneracy of that of the GS transition[26]. However, the measured RT PC of the samples reported here shows the first ES to have its peak *below* that of the GS. Additionally, for a QD ensemble with linewidths of ≈28meV and GS-ES splitting of 85meV, there should be essentially zero absorption between the states. However it is noted that there is a clear signal at ≈1.02eV, Gaussian fitting of the GS and ES transitions fails to accurately describe this region.

In order to understand the observed PC spectrum, the shape of the DoS is calculated by summing and energy binning the first 6 parity conserving energy transitions, which are the electron-hole transitions, whose quantum number transitions are; 111, 211, 121, 221, 131, 311 (as previously described), using the QD shape distributions as described previously. All transitions are assumed to have the same oscillator strength and none of the forbidden states are considered. Additionally continuum-bound and bound-continuum transition will occur to higher energies. At high energies our model will break down due to the assumption of infinite barriers so higher order transitions are not considered. The results of these calculations produces an excellent agreement to the shape of the PC spectra. Showing that with the limitations of the infinite barriers model an agreement

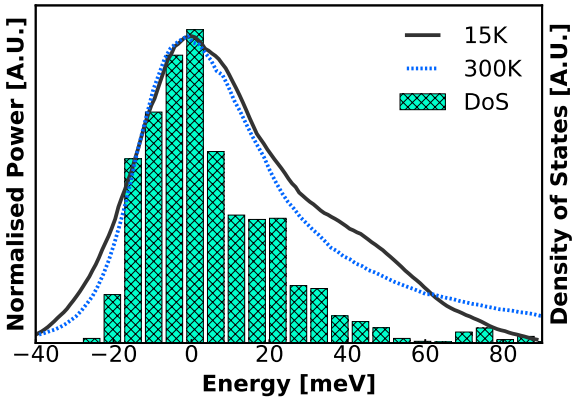

FIG. 2: Calculated shape of density of states for measured QD size distributions, and EL at 15K and 300K. Energy is plotted relative to peak energy to allow comparison at different temperatures.

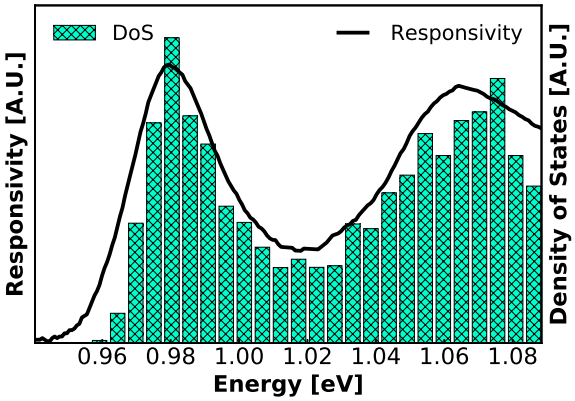

FIG. 3: Room temperature (∼300K) PC responsivity, using an applied bias of 0V, and calculated shape of the absorption spectrum for the first 6 allowed optical transitions.

is shown only using the lower order transitions. The widths, separations and relative heights of the peaks also the magnitude of absorption/DoS between the peaks are all well described by the model.

Inhomogeneity in QDs is known to be directly linked to the broadening of the lasing linewidth. Improving the inhomogeneous linewidth, close to the homogeneous linewidth will see vast improvement of devices[30,31]. While significant work has already been completed[15], we have identified that inhomogeneity is more pronounced in one crystallographic direction, suggesting further development needs to be completed in solving this anisotropic broadening, leading to next generation of QD laser epitaxy.

Modulation rate, laser differential efficiency and even output power will improve as GS saturated gain (G_{sat}) increases. In order to explore possible increases in GS G_{sat} we simulate the shape of the DoS of the ensemble for GS. Making changes to the distributions the DoS shape can be compared between different ensembles. The anisotropic QDs from Fig. 1 can be compared to an isotropic ensemble by setting both orthogonal size distributions as the narrower major flat distribution.

Figure 4 plots the simulated shape of the ensemble DoS for these two situations for the lowest energy allowed transition, mimicking the emission properties of the QD ensemble after EL in figure 2. In this case, the linewidth is narrowed from 32meV (± 2meV) to 16meV (± 2meV). A 40% enhancement in the peak DoS is observed, suggesting G_{sat} may be increased by the same amount, which would result in a ≈20% increase in K-factor limited modulation bandwidth[32].

The inset to Figure 4 shows the effect of reducing the inhomogeneity in the minor flat direction on the absorption spectrum, by plotting the shape of the DoS for the first 6 parity conserving optical transitions as performed for figure 3. In addition to the narrowing of the GS transition, the excited state transition is also shown to be narrowed. Interestingly, essentially zero absorption is observed between the GS and ES peaks. This is particularly important in realising a electro-absorption modulated laser with negative chirp[33,34]. We also note that enhancing this asymmetry may allow broadband emitter to be realised as the increasing degeneracy of higher energy states poses a limitation for QD broadband emitters[35].

In summary, we have described a TEM study of QD laser sample. The sample is shown to have an anisotropy in the inhomogeneity of the QD size distribution. This results in the shape of the DoS being altered as compared to the case of size isotropy. Measured EL and RT PC spectra are in very good agreement with a simulation of the shape of the DoS that uses our structural measurements to describe the size distribution of the QD ensemble. This model could be integrated in a Monte-carlo simulation enabling structural analysis in simulating gain spectra. Our results suggest that in order to further improve QD laser devices, this newly identified inhomogeneity along (110) should be the focus of epitaxial process development. The impact of achieving a size inhomogeneity of (110) that can match that of ($\bar{1}$10) on device performance was discussed. Additionally, prospects for advanced electro-absorption modulator (EAM) lasers may be made possible by such developments.

ACKNOWLEDGMENTS

This work was supported by the Engineering and Physical Sciences Research Council (RCUK Grant No. EP/L015323/1).

[1] N. Kirstaedter, M. Grundmann, U. Richter, V. Ustinov, P. Kop'ev, D. Bimberg, P. Werner, S. Ruvimov, N. Ledentsov,

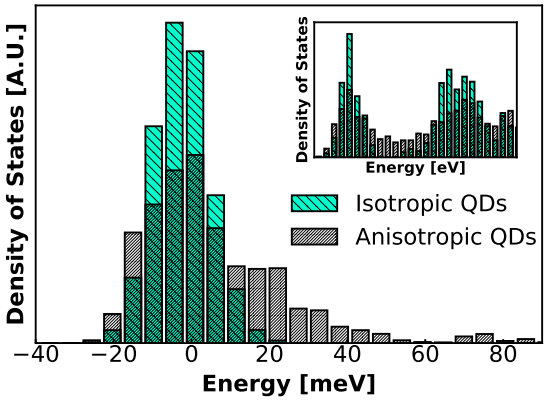

FIG. 4: A comparison of the shapes of ground state density of states anisotropic and isotropic as described in text. Inset shows calculated absorption spectrum for the same two size distributions.

U. Gsele, Z. Alferov, J. Heydenreich, and M. Maximov, Electronics Letters **30**, 1416 (1994).

[2] Y. Arakawa and H. Sakaki, Applied Physics Letters **40**, 939 (1982), http://dx.doi.org/10.1063/1.92959.

[3] S. Fathpour, Z. Mi, P. Bhattacharya, A. R. Kovsh, S. S. Mikhrin, I. L. Krestnikov, A. V. Kozhukhov, and N. N. Ledentsov, Applied Physics Letters **85**, 5164 (2004), http://dx.doi.org/10.1063/1.1829158.

[4] K. Otsubo, N. Hatori, M. Ishida, S. Okumura, T. Akiyama, Y. Nakata, H. Ebe, M. Sugawara, and Y. Arakawa, Japanese Journal of Applied Physics **43**, L1124 (2004).

[5] K. Nishi, T. Kageyama, M. Yamaguchi, Y. Maeda, K. Takemasa, T. Yamamoto, M. Sugawara, and Y. Arakawa, Journal of Crystal Growth **378**, 459 (2013).

[6] E. Clarke, P. Spencer, E. Harbord, P. Howe, and R. Murray, Journal of Physics: Conference Series **107**, 012003 (2008).

[7] Z. Y. Zhang, A. E. H. Oehler, B. Resan, S. Kurmulis, K. J. Zhou, Q. Wang, M. Mangold, T. Süedmeyer, U. Keller, K. J. Weingarten, and R. A. Hogg, Scientific Reports **2** (2012), 10.1038/srep00477.

[8] D. L. Huffaker, G. Park, Z. Zou, O. B. Shchekin, and D. G. Deppe, Applied Physics Letters **73**, 2564 (1998).

[9] R. R. Alexander, D. T. D. Childs, H. Agarwal, K. M. Groom, H. Y. Liu, M. Hopkinson, R. A. Hogg, M. Ishida, T. Yamamoto, M. Sugawara, Y. Arakawa, T. J. Badcock, R. J. Royce, and D. J. Mowbray, IEEE Journal of Quantum Electronics **43**, 1129 (2007).

[10] Z. Mi, J. Yang, P. Bhattacharya, and D. Huffaker, Electronics Letters **42**, 121 (2006).

[11] K. Nishi, K. Takemasa, M. Sugawara, and Y. Arakawa, IEEE Journal of Selected Topics in Quantum Electronics **23**, 1 (2017).

[12] K. Brunner, U. Bockelmann, G. Abstreiter, M. Walther, G. Bhm, G. Trnkle, and G. Weimann, Physical Review Letters **69**, 3216 (1992).

[13] K. Nishi, H. Saito, S. Sugou, and J.-S. Lee, Applied Physics Letters **74**, 1111 (1999).

[14] P. W. Fry, I. E. Itskevich, D. J. Mowbray, M. S. Skolnick, J. J. Finley, J. A. Barker, E. P. O'Reilly, L. R. Wilson, I. A. Larkin, P. A. Maksym, M. Hopkinson, M. Al-Khafaji, J. P. R. David, A. G. Cullis, G. Hill, and J. C. Clark, Physical Review Letters **84**, 733 (2000).

[15] T. Yang, J. Tatebayashi, S. Tsukamoto, M. Nishioka, and Y. Arakawa, Applied Physics Letters **84**, 2817 (2004).

[16] C. Ngo, S. Yoon, W. Fan, and S. Chua, in *2006 International Conference on Numerical Simulation of Semiconductor Optoelectronic Devices* (IEEE, 2006).

[17] R. Ferreira, in *Capture and Relaxation in Self-Assembled Semiconductor Quantum Dots: The dot and its environment* (IOP Publishing, 2015).

[18] T. Walther, A. G. Cullis, D. J. Norris, and M. Hopkinson, Phys. Rev. Lett. **86**, 2381 (2001).

[19] P. Wang, A. L. Bleloch, M. Falke, P. J. Goodhew, J. Ng, and M. Missous, Applied Physics Letters **89**, 072111 (2006).

[20] T. Inoue, T. Kita, O. Wada, M. Konno, T. Yaguchi, and T. Kamino, Applied Physics Letters **92**, 031902 (2008).

[21] M. Grundmann and D. Bimberg, Physical Review B **55**, 9740 (1997).

[22] N. Peyvast, H. Shahid, R. A. Hogg, and D. T. D. Childs, Applied Physics Express **8**, 122102 (2015).

[23] T. V. Hakkarainen, A. Schramm, J. Tommila, and M. Guina, Journal of Applied Physics **111**, 014306 (2012), http://dx.doi.org/10.1063/1.3675271.

[24] H. Li, Q. Zhuang, Z. Wang, and T. Daniels-Race, Journal of Applied Physics **87**, 188 (2000).

[25] J. M. Garcia, G. Medeiros-Ribeiro, K. Schmidt, T. Ngo, J. L. Feng, A. Lorke, J. Kotthaus, and P. M. Petroff, Applied Physics Letters **71**, 2014 (1997).

[26] S. A. Sobhani, D. T. Childs, N. Babazadeh, B. J. Stevens, K. Nishi, M. Sugawara, K. Takemasa, and R. A. Hogg, in *Physics and Simulation of Optoelectronic Devices XXIV*, edited by B. Witzigmann, M. Osiński, and Y. Arakawa (SPIE, 2016).

[27] T. Ishihara, S. Lee, M. Akabori, J. Motohisa, and T. Fukui, Journal of Crystal Growth **237-239**, 1476 (2002).

[28] N. Peyvast, K. Zhou, R. A. Hogg, and D. T. D. Childs, Applied Physics Express **9**, 032705 (2016).

[29] G. Saint-Girons, G. Patriarche, L. Largeau, J. Coelho, A. Mereuta, J. M. Moison, J. M. Gérard, and I. Sagnes, Applied Physics Letters **79**, 2157 (2001), http://dx.doi.org/10.1063/1.1406553.

[30] L. V. Asryan and R. A. Suris, Semiconductor Science and Technology **11**, 554 (1996).

[31] M. Sugawara, K. Mukai, Y. Nakata, H. Ishikawa, and A. Sakamoto, Physical Review B **61**, 7595 (2000).

[32] B. J. Stevens, D. T. D. Childs, H. Shahid, and R. A. Hogg, Applied Physics Letters **95**, 061101 (2009).

[33] K. Morito, R. Sahara, K. Sato, and Y. Kotaki, IEEE Photonics Technology Letters **8**, 431 (1996).

[34] R. Sahara, M. Matsuda, H. Shoji, K. Morito, and H. Soda, IEEE Photonics Technology Letters **8**, 1477 (1996).

[35] S. Chen, K. Zhou, Z. Zhang, J. R. Orchard, D. T. D. Childs, M. Hugues, O. Wada, and R. A. Hogg, IEEE Journal of Selected Topics in Quantum Electronics **19**, 1900209 (2013).